

UC San Diego

UC San Diego Previously Published Works

Title

Assessment of approaches to obtain ebullition pressures for organophilic clay blankets

Permalink

<https://escholarship.org/uc/item/38q4t5xx>

Journal

Geosynthetics International, 26(5)

ISSN

1072-6349

Authors

Eun, J
McCartney, JS
Znidarčič, D

Publication Date

2019-10-01

DOI

10.1680/jgein.19.00042

Peer reviewed

2 **ASSESSMENT OF APPROACHES TO OBTAIN EBULLITION PRESSURES FOR ORGANOPHILIC CLAY**
3 **BLANKETS**

4
5 **Abstract:** The objective of this study is to compare two experimental approaches to characterize
6 the ebullition pressure (or air-entry suction) of initially water-saturated organophilic clay blankets.
7 The first is an indirect approach using the water-retention curve (WRC) and the second is a direct
8 approach using ebullition experiments. The WRC along with the hydraulic conductivity of
9 organophilic clay blankets in saturated and unsaturated conditions were measured using a flexible-
10 wall permeameter with suction-saturation control. This device was also adapted to measure the
11 ebullition pressure and the air permeability. The comparison of the experimental approaches was
12 performed on organophilic clay blanket specimens in different initial conditions (unrinsed and
13 rinsed to remove loose fines) under high and low effective confining stresses (20 and 5 kPa). The
14 indirect estimates of air-entry suction from the WRC were similar to those obtained from the
15 ebullition tests. This good agreement between the two approaches may add flexibility to the
16 development of design specifications for capping systems. The hydraulic properties were found to
17 be sensitive to rinsing and effective stress, with greater hydraulic conductivity and air permeability
18 for the rinsed specimen due to the removal of fines, and greater air-entry suctions for specimens
19 under higher effective stress.

20 **KEYWORDS:** Geosynthetics, organophilic clay blankets, gas ebullition, air-entry, water
21 retention curve

22 **AUTHORS:** Jongwan Eun, Ph.D., P.E., Assistant Professor, Univ. of Nebraska-Lincoln, Dept. of
23 Civil Engineering, Lincoln, NE 68588-6105; Email: jeun2@unl.edu. Telephone: 1-402-554-3544.

24 J.S. McCartney, Ph.D., P.E., F.ASCE, Professor and Department Chair, Univ. of California San
25 Diego, Dept. of Structural Engineering, 9500 Gilman Dr., La Jolla, CA 92093-0085. E-mail:
26 mccartney@ucsd.edu. Telephone: 1/858-534-9630. D. Znidarčič, Ph.D., Professor, Univ. of
27 Colorado Boulder, Dept. of Civil, Architectural and Environmental Engineering, Boulder, CO
28 80309-0428; E-mail: znidarci@colorado.edu. Telephone: 1/303-492-7577.

29 **DATES:** Original manuscript submitted October 30, 2018, accepted _____. Discussion open
30 until _____.

31 **REFERENCE:** Eun, J., McCartney, J.S. and Znidarčič, D. 2018, "Evaluation of gas ebullition
32 through organophilic clay blankets." Geosynthetics International, Vol. __, No. __, pp. ____ - ____.

33

INTRODUCTION

Sediment capping has been shown to be a more effective, economic, and durable in-situ treatment to stabilize and remediate contaminated subaqueous sediments in lakes or rivers compared to ex-situ methods such as dredging (Locate et al. 2003; Reible et al. 2003, 2006; Yuan et al. 2007, 2009; Olsta 2010; Perele 2010; Eun et al. 2012a,b; Ebrahimi et al. 2014, 2016; Zhang et al. 2016; Gu et al. 2017). From 1990 to 2006, approximately six million cubic meters of contaminated sediment have been removed and disposed of through the implementation of 71 major environmental remediation projects in the United States (Zeller and Cushing 2006). In addition to potentially mobilizing organic contaminants in surface waters, the dredged sediments must be treated or disposed of in another containment system. Sediment capping systems on the other hand are intended to contain the contaminants in-situ.

Early sediment capping systems involved several layers of granular material placed atop the contaminated sediment. However, an issue identified is that sand caps may lead to consolidation of the contaminated sediments, releasing contaminants from the sediment without a means of fixing them (Alshawabkeh et al. 2005). An alternative lightweight capping system used to confine contaminated sediments in lakes or rivers with a means of fixing released contaminants is shown in Figure 1(a). This system involves an organophilic clay blanket overlain by a surcharge layer of porous geomaterial (typically sand) and an armor layer (typically gravel) to prevent scour. The organophilic clay blanket contains sodium bentonite whose interlayer cations were exchanged with organocations to absorb organic contaminants. The treated sodium bentonite particles are hydrophobic and are different from untreated sodium bentonite that in the presence of water they will not hydrate and will remain inert like sand particles. However, they will absorb organic liquids and swell. The treated sodium bentonite particles are encapsulated between geotextiles that are

57 needle-punched together for ease of transport and placement. The intention of the composite
58 blanket is to provide a permeable but lightweight (thin) composite material that can be placed
59 underwater to replace a thicker and heavier sand cap.

60 Sediment capping systems are intended to be water-permeable so as not to disturb the sediment
61 during changes in water flow. However, a risk is that gases such as methane can be generated from
62 the decomposition of organic matter in the sediment or other mechanisms and then become trapped
63 beneath the organophilic clay blanket. Specifically, gas from the sediments will tend to move
64 upward due to buoyancy but will not pass through the layers in the capping system until the gas
65 pressure exceeds the gas-entry pressure of the different layers. The breakthrough of gas into an
66 initially saturated media is referred to as ebullition, and the air-entry suction is often referred to as
67 the ebullition pressure. Even after breakthrough at a given location, gas may accumulate in the
68 case that gas generation rates are greater than the gas flow rate through the capping system.
69 Without sufficient gas transport through a sediment capping system, uplift failure may occur if
70 the pressure in the gas trapped beneath the capping system exceeds the total overburden stress
71 (Mohan et al. 2000; Alshawabkeh et al. 2005; Paul et al. 2005; McLinn and Stolzenburg 2009a,
72 2009b; Chattopadhyay et al. 2010; Eun et al. 2012b). An example of a sediment capping system
73 that failed by uplift is shown in Figure 1(b).

74 The primary objective of this study is to compare the air-entry suctions of initially water-
75 saturated organophilic clay blankets obtained from indirect and direct approaches to provide a
76 wider range of options for engineers when developing design specifications for capping systems
77 incorporating organophilic clay blankets. The indirect approach involves estimation of the air-
78 entry suction from the water retention curve (WRC) of the organophilic clay blanket under
79 different effective confining stresses. The direct approach involves ebullition experiments where

the air pressure is gradually increased to the boundary of an initially water-saturated organophilic clay blanket until breakthrough occurs. The advantage of using an indirect approach is that the testing procedures to determine the WRC of geosynthetic materials are well established in the literature (Nahlawhi et al. 2009; McCartney and Zornberg 2010; Zornberg et al. 2010) and are easier to perform reliably than ebullition experiments. In this study, the WRCs of organophilic clay blankets were measured using a flexible wall permeameter device described by McCartney and Znidarčič (2010). This device also permits measurement of the hydraulic conductivity function (HCF), which is inversely related to the gas permeability as the degree of saturation of the organophilic clay blanket changes. This device was also modified to directly measure the ebullition pressures and air permeability of organophilic clay blankets. The tests associated with the indirect and direct approaches were repeated for an organophilic clay blanket in the as-received condition under a higher effective stress of 20 kPa to represent a likely situation in the field, and a organophilic clay blanket rinsed with tap water to simulate the removal of loose fines during placement under a lower effective stress of 5 kPa to represent the effects of a thin overburden layer or scour of the armor layer.

BACKGROUND

Organophilic Clay Blankets

Organophilic clay blankets are manufactured in a similar manner to geosynthetic clay liners and consist of a layer of organophilic clay (i.e., an active or adsorptive media suitable for capture of organic contaminants), encapsulated between geotextiles that are needle-punched together. Organophilic clay is a coarse material before reacting with organic contaminants such as light non-aqueous phase liquids (Erten et al. 2012; Benson et al. 2015). Depending on the contaminant present in the sediment layer, other materials like Granular Activated Carbon, Attapulgite, Apatite,

or Zeolites, can be included to “fix” or absorb contaminants which are carried from the sediments by advective or diffusive flow. Although this study is focused on the gas ebullition and permeability behavior of organophilic clay blankets, similar gas ebullition problems may be encountered with these other fixing materials. Accordingly, a goal of this study is to evaluate methods to determine the ebullition pressure and hydraulic properties that may be extended to evaluate organophilic blankets created with these other fixing materials.

Hydraulic Properties of Unsaturated Geomaterials

When gas ebullition occurs, the organophilic clay blanket will become unsaturated. Accordingly, it is relevant to understand the hydraulic properties of organophilic clay blankets under both saturated conditions (i.e., before gas entry) and unsaturated conditions (i.e., after gas entry). Specifically, it is well known that the air-entry suction for a geomaterial is related to the shape of its water retention curve (WRC), which describes the water storage in the geomaterial as a function of the matric suction (the difference between the pore air and pore water pressures in an unsaturated geomaterial). It is common to determine equilibrium points on a WRC using one or more techniques described in ASTM D6836 or ASTM D7664, then fit a continuous function to these points. The most commonly used continuous function for the WRC is the model of van Genuchten (1980), given as follows:

$$S_e = \left(\frac{1}{1 + (\alpha_{vG} \psi)^{n_{vG}}} \right)^m \quad (1)$$

where S_e is the effective saturation equal to $\frac{S - S_{res}}{1 - S_{res}}$, S is the degree of saturation, S_{res} is the degree of saturation at residual conditions, ψ is the matric suction, α_{vG} and n_{vG} are fitting parameters specific to a given material, and $m = (1 - 1/n_{vG})$. The parameter α_{vG} is related to the inverse of the air-entry suction of the geomaterial and the parameter n_{vG} is related to the pore size distribution of the geomaterial.

Water flow through an unsaturated organophilic clay blanket is assumed to be governed by Darcy's law with a hydraulic conductivity value that depends on the effective saturation. The hydraulic conductivity of unsaturated organophilic clay blankets is inversely related to the gas permeability; the gas permeability reaches a maximum value when the hydraulic conductivity approaches a minimum value, and vice-versa. Nahlawi et al. (2007), Zornberg et al. (2010) and McCartney and Zornberg (2010) showed that the unsaturated hydraulic conductivity (k) of nonwoven geotextiles can be predicted from the parameters of the WRC in Eq. (1) using the van Genuchten-Mualem hydraulic conductivity function (HCF) (Mualem 1976; van Genuchten 1980). The van Genuchten-Mualem HCF is given as follows:

$$k(S_e) = k_{sat} \cdot S_e^\tau \left[1 - (1 - S_e^{\frac{1}{m}})^m \right]^2 \quad (2)$$

where k_{sat} is the hydraulic conductivity at saturated conditions, τ is a tortuosity factor equal to 0.5 (Mualem 1976), and m is the value obtained from fitting Eq. (1) to experimental WRC data. McCartney and Zornberg (2010) observed that the hydraulic conductivity of an unsaturated nonwoven geotextile decreased from 9.0×10^{-1} to 7.0×10^{-10} m/s for matric suction values increasing from 0.1 to 2.5 kPa. This trend in the hydraulic conductivity implies that in this matric suction range the gas permeability of organophilic clay blankets will increase rapidly after reaching the air-entry suction.

MATERIALS AND METHODS

Organophilic Clay Blanket Specimens

The organophilic clay blanket evaluated in this study was a Reactive Core Mat[®] obtained from CETCO[®] and consisted of a layer of Organoclay[®] sandwiched between a nonwoven cap geotextile and a nonwoven carrier geotextile, as shown in Figure 2. The two geotextiles were needle punched together. The initial height of the blanket was 6 mm. The properties of the carrier geotextiles in

the organophilic clay blanket are summarized in Table 1. The particle size distribution of organophilic clay ranged from 0.09 to 2.50 mm based on a dry mechanical sieve analysis with characteristic particle sizes D_{30} of 0.56 mm and D_{60} of 0.72 mm, and a coefficient of uniformity C_u of 1.29. The particle size of the organophilic clay is relatively coarse, like a sandy soil. As mentioned, due to the chemical treatment of the smectite during manufacturing, the organophilic clay is nonreactive with water and is expected to have a relatively high hydraulic conductivity approaching that of sand. When the organophilic clay encounters organic contaminants, it will absorb the organic contaminants, swell, and experience a reduction in permeability. The specific gravity of the organophilic clay particles is 1.75, which is lighter than most soils.

Specimen Preparation

To prepare specimens for testing, the organophilic clay blanket in as-received conditions was compressed tightly against a plastic sheet using a steel cylinder having a diameter of 65 mm, which is the target diameter of the specimen. A razor blade was then used to trim around the edges of the cylinder to form the specimen. This approach was observed to lead to a well-defined circular specimen with minimal loss of the organophilic clay from the edges. Two different types of organophilic clay blanket specimens were prepared: a specimen in the as-received condition which represents the likely initial state for an organophilic clay blanket deployed in the field, and a specimen rinsed thoroughly in tap water to wash away any loose fines. The rinsed specimen was used to simulate an organophilic clay blanket that has had long-term interaction with water flow. The as-received specimen was tested under a relatively high effective confining stress of 20 kPa, while the rinsed specimen was tested under a lower overburden pressure to simulate a thin overburden layer or the case where the overburden and armor layers had eroded over time.

Flexible Wall Permeameter System

The different tests on organophilic clay blankets in this study were performed using a flexible wall permeameter system developed by McCartney and Znidarčić (2010) shown in Figure 3. Although this system was originally developed to measure the hydraulic properties of saturated and unsaturated geosynthetics, it was also adapted in this study to perform ebullition and air permeability tests. A rigid wall permeameter was investigated in preliminary ebullition tests as part of this study, but sidewall leakage through the gap between the specimen and the wall of a rigid wall permeameter was observed. In addition to minimizing the effect of sidewall leakage, the flexible wall permeameter permits backpressure saturation of the specimens along with careful control of effective stress and changes in height. Unsaturated conditions can be controlled in the flexible wall permeameter system using the axis translation technique, which involves use of a high air-entry porous membrane to apply air and water pressures independently to a specimen. The pressure difference across the specimen is measured using a differential pressure transducer (model P55E from Validyne), which can measure both water and air pressures. The accuracy of the differential pressure transducer is $\pm 0.1\%$, and a diaphragm was used in the transducer to permit measurement of differential pressures as small as 0.01 kPa. The air and water pressures can be applied using a pressure control panel. In addition, a flow pump connected to the bottom platen of the permeameter can be used to apply constant water pressures to the specimen while tracking outflow in WRC and HCF tests on unsaturated specimens, or to apply constant flow rates in hydraulic conductivity tests on saturated specimens. The measurements from the differential pressure transducer can be used to operate the pump in pressure-control mode. In ebullition testing, the air pressure can be applied using the pressure control panel, and after breakthrough air flow rates can be measured by transferring air from one reservoir to another. Alternatively, constant air

flow rates may be imposed after reaching the ebullition pressure using a mass flow controller from MKS Instruments. More details of the mass flow controller are given in Alsherif and McCartney (2015).

Water Retention Curves

Equilibrium points on the WRC of the organophilic clay blanket specimen were measured using the flexible permeameter device and the flow pump operating in suction-control mode. Although this technique is not covered in ASTM D6836 for determination of the WRC, it is consistent with Method B2 in ASTM D7664 for joint determination of the WRC and HCF. In the axis translation technique, the matric suction applied to a specimen is equal to the difference between the pore air and pore water pressures. Specifically, the air pressure applied to the upper side of the specimen is greater than the water pressure applied to the bottom side of the specimen. It is possible to independently apply pore air and pore water pressures to a specimen by placing a high air-entry porous membrane on the water-side of the specimen. Although other high air-entry porous materials like sintered clay may be used in the axis translation technique, McCartney and Znidarcic (2010) found that the use of a thin porous membrane provides less impedance to outflow from the specimen during hydraulic property measurements. The porous membrane used in this study is a cellulose sheet having a thickness of 0.05 mm and an air-entry suction of approximately 100 kPa. When saturated with water, the high air-entry porous membrane only permits the passage of water until the difference in the air and water pressures across the specimen reaches 100 kPa.

Backpressure saturation was used to initially saturate the organophilic clay blanket specimen with tap water within the flexible wall permeameter. After saturation of the specimen under a backpressure of 330 kPa, the specimen was consolidated to a desired initial effective confining stress (e.g., a cell pressure of 350 kPa and a backpressure of 330 kPa to apply an effective confining

stress σ' of 20 kPa on the un-rinsed specimen and a cell pressure of 350 kPa and a backpressure of 345 kPa to apply an effective confining stress σ' of 5 kPa to the rinsed specimen). The water was then flushed from the top side of the specimen so that the air pressure at the top of the specimen was equal to the water backpressure applied to the bottom side of the specimen (i.e., no flow condition).

The flow pump was then used to extract water from the bottom of the specimen in stages to reach different target suction values following the approach of Znidarčič et al. (1991) and McCartney and Znidarčič (2010). To measure different equilibrium points on the WRC, a flow pump is used to control the volume of water extracted from an initially-saturated specimen. The flow pump is operated in suction-control model and applies a constant volumetric flow rate from the specimen until a target suction is reached, which is measured using the differential pressure transducer connected to the top and bottom of the specimen (i.e., the difference in the air pressure and the water pressure on across the specimen). An encoder on the pump is used to measure the volume of water extracted from the specimen can be used to directly calculate the degree of saturation of the specimen.

After the suction measured by the differential pressure transducer reaches a target suction value, the suction inside the specimen may not be in equilibrium with this value. Specifically, the suction measured using the differential pressure transducer is only applicable to the boundaries of the specimen. The suction inside the specimen may take some time to reach hydraulic equilibrium with the suction value applied at the boundary. Accordingly, a feedback-control loop was used to operate the flow pump until reaching equilibrium under different target suction values. After reaching a target suction value, the flow pump is stopped and the suction at the boundaries of the specimen is then monitored using the differential pressure transducer. If the suction in the

specimen is not in equilibrium with the suction imposed at the specimen boundaries, water will flow toward the outflow face and the suction measured by the differential pressure transducer will decrease. If the measured suction decreases below a threshold value (i.e., 0.16 kPa lower than the target suction), the pump is operated again to draw more water from the specimen and bring the suction at the specimen boundaries back to the target suction. This iterative process is repeated until the measured suction at the specimen boundaries does not drop below the outflow face over the span of 5000 seconds (a time period selected by experience to signify equilibrium. At this point the suction within the specimen is assumed to be in equilibrium with the applied suction at the boundary of the specimen induced by the flow pump operation. The cumulative amount of water withdrawn from the specimen during this iterative process corresponds to the change in the degree of saturation of the specimen during each suction increment. After reaching equilibrium, the next value for the target suction is applied and the iterative process is repeated. After reaching the maximum target suction, the final volume was measured, the specimen was unloaded, and the final gravimetric water content was measured. Only the drying path WRC was investigated in this study due to the focus on the characterization of the air-entry suction.

Hydraulic Conductivity Function

Points on the HCF of the unsaturated organophilic clay blankets can be inferred from the outflow data from the WRC test. Specifically, the outflow data measured when applying a given suction value as part of reaching an equilibrium point on the WRC were analyzed using the approach described in ASTM D7664 method B2 (i.e., a multi-step outflow test with outflow data analyzed using Gardner's method). Gardner's method involves normalizing the curve of water outflow versus time for each suction value applied by plotting $\ln[(V_f - V)/V_f]$ versus time, where V is the outflow at a given moment in time and V_f is the final amount of outflow for a given suction

increment. The slope of the normalized outflow as a function of time is directly proportional to the diffusivity D , which can be calculated as the slope multiplied by $4H^2/\pi^2$, where H is the specimen height. The diffusivity can then be used to calculate the hydraulic conductivity as follows,

$$k = D \frac{\Delta\theta}{\Delta\psi} \gamma_w \quad (3)$$

where k is the hydraulic conductivity of an unsaturated specimen, θ is the volumetric water content, $d\theta/d\psi$ is the slope of the WRC plotted in terms of the volumetric water content corresponding to the applied increment in suction, and γ_w is the unit weight of water.

Determination of the Air Permeability

The flexible-wall permeameter used to measure the hydraulic properties of the organophilic clay blankets was also adapted to measure the ebullition pressure and air permeability. Specifically, the same setup was used but without a high air-entry porous membrane. First, the organophilic clay blanket was back-pressure saturated with water after which the hydraulic conductivity was calculated from Darcy's law by applying a constant flow rate through the specimen and measuring the gradient across the blanket using a differential pressure transducer. Next, the water was flushed from below the blanket with air. The air pressure was then gradually increased in small increments until breakthrough occurred. This was identified as the ebullition pressure.

The air permeability was measured using different methods for the two specimens tested. For the unrinsed specimen under an effective confining stress of $\sigma' = 20$ kPa, the average air flow volume passing through the blanket over time was measured for a constant applied pressure difference. Specifically, the volume of air passing through the specimen was monitored over time by passing air from one reservoir to the other in the pressure control panel. The air permeability k_a was then calculated as follows:

$$k_a = \left(\frac{Q_{AV}}{\Delta P} \frac{H}{A} \mu \right) \times \left(10^{12} \frac{\text{darcy}}{\text{m}^2} \right) \quad (4)$$

where Q_{av} is the average volumetric flow rate of air, H is the height of the specimen, A is the specimen area, μ is the dynamic viscosity of air, and ΔP is the applied air pressure difference. The value of H for the unrinsed specimen was 0.006 m, A was 0.003 m², and μ was 1.82×10⁻⁸ kPa·s. In the test on the rinsed specimen under an effective confining stress $\sigma' = 5$ kPa, the mass flow controller was used to apply a constant air flow rate across the specimen (after reaching the gas breakthrough pressure). The air pressure difference corresponding to this constant flow rate was then measured using the differential pressure transducer and the air permeability was calculated using Eq. (4). This approach was found to lead to more stable results than the other method and permits an evaluation of changes in air permeability for a range of gas flow rates.

HYDRAULIC PROPERTIES OF ORGANOPHILIC CLAY BLANKETS

Hydraulic Conductivity of Saturated Organophilic Clay Blankets

The variation of hydraulic conductivities with time obtained from the flexible wall tests on the unrinsed and rinsed specimens under effective confining stresses of 20 and 5 kPa are shown in Figure 4. These results were obtained from the initial portion of the air permeability tests, where no high air-entry porous membrane was included to affect the flow process. The hydraulic conductivity of the unrinsed specimen ranged from 3.6×10^{-5} m/s to 3.2×10^{-6} m/s over time. The hydraulic conductivity was observed to continuously decrease during steady water flow through the saturated specimen, which is likely due to redistribution of the organophilic clay particles within the blanket. The test was stopped after approximately 4 days as a stable hydraulic conductivity value was not reached. For the rinsed specimen, the hydraulic conductivity ranged from 1.0×10^{-4} to 3.0×10^{-5} m/s, with a slightly lower decrease in hydraulic conductivity over time. The order of magnitude greater hydraulic conductivity range measured for the rinsed

specimen is attributed to both the rinsing process (which removed loose fine particles) and the lower effective confining stress (which leads to lower compression of the specimen).

The system hydraulic conductivity of the saturated organophilic clay blanket atop the porous membrane was also measured to evaluate the impact of the porous membrane on the hydraulic conductivity. Specifically, at the beginning of the WRC tests, the hydraulic conductivity was calculated from Darcy's law using the applied flow rate across the saturated assembly and the measured pressure gradient across the specimen and the membrane. It was found that a relatively high flow rate of 0.02 ml/s was required to establish a stable gradient, as shown in Figure 5 for the test on the unrinsed specimen. The average hydraulic conductivity of the system ranged from 1.3×10^{-6} to 9.0×10^{-7} m/s. The hydraulic conductivity values in Figure 4(a) for the assembly including the porous membrane are two orders of magnitude lower for the organophilic clay blanket without a membrane. Although the porous membrane is very thin (0.05 mm), it does provide impedance to outflow.

Outflow Measurement from Organophilic Clay Blankets

The transient outflow during application of different suction increments is shown in Figure 6(a) and 6(b) for the unrinsed and rinsed specimens, respectively. The results in these figures show that longer equilibrium times were required for the lower matric suction values, and that progressively shorter times were required for the higher matric suction values. This is because the most water was extracted at a suction of 3-4 kPa. Approximately 20 ml was withdrawn from the unrinsed specimen under a higher effective confining stress of 20 kPa after reaching a suction of approximately 16 kPa, while a greater amount of approximately 31 ml was withdrawn from the rinsed specimen under a lower effective stress of 5 kPa after reaching a suction of approximately

15 kPa. The greater outflow for the rinsed specimen is due to the higher porosity of the specimen associated with the lower effective confining stress.

Next, the outflow from the specimen due to the application of a given suction increment was transformed using Gardner's method, as shown in Figures 7(a) and 7(b) for the unrinsed and rinsed specimens, respectively. These normalized outflow curves were used to estimate the diffusivity values when calculating the hydraulic conductivity for each suction increment. The portions of the curves that are relatively linear before the steep drop were used to calculate the slope used in the diffusivity calculation.

Water Retention Curves of Organophilic Clay Blankets

The WRCs were calculated by first converting the outflow data to the degree of saturation using the thickness of the specimens under the applied effective confining stresses, then plotting this against the measured matric suction values in Figure 6. The WRC for the unrinsed specimen is shown in Figure 8(a) and the WRC for the rinsed specimen is shown in Figure 8(b), with circles denoting the equilibrium points at each applied matric suction value. The overall porosity of the unrinsed organophilic clay blanket was estimated to be 0.97, which is slightly lower than that of the nonwoven carrier geotextiles. The use of this porosity value corresponded well with the volume of water extracted from the specimen during the WCR test. The van Genuchten (1980) WRC model (Eq. 1) was fitted to the equilibrium points on the primary drainage (drying) path of the WRC. The parameters used to fit the model to the data are listed in Table 2. These parameters are consistent with those measured for geosynthetics (McCartney and Znidarčić 2010) and are similar to those of a coarse sand (Znidarčić et al. 1991).

The most important value on the WRC for the purposes of gas flow through organophilic clay blankets is the air-entry suction (ψ_a), which is defined as the suction at which air starts to displace

water in an initially saturated organophilic clay blanket. The air-entry suction from the WRC for the unrinsed specimen in Figure 8(a) is approximately 0.68 kPa, while the air-entry suction from the WRC for the rinsed specimen in Figure 8(b) is approximately 0.60 kPa. A comparison of the fitted WRCs for the unrinsed and rinsed specimens is shown in Figure 8(c). The lower air-entry suction for the rinsed specimen is primarily attributed to the lower effective confining stress because rinsing likely only removed the fine particles. The fine particles are expected to affect the shape of the WRC at high suctions. Higher effective confining stresses are expected to compress the voids of the organophilic clay blanket, leading to a smaller pore size distribution and a shift in the WRC to the right that causes the air-entry suction to increase. However, the impact of effective confining stress on the air-entry suction is not so significant that the risk of uplift failure would increase (i.e., the increase in the air entry suction is much smaller than the increase in the effective confining stress).

Hydraulic Conductivity Functions of Organophilic Clay Blankets

The HCF data for the unrinsed and rinsed organophilic clay blanket under effective stresses of 20 and 5 kPa are shown in Figures 9(a) and 9(b), respectively. The HCF data shows some scatter due to the variability in the outflow curves for the different suction values, but overall a clear decreasing trend with increasing suction is observed as expected. The effect of the high air-entry porous membrane on the system hydraulic conductivity was not removed from the data, although it can be assumed that the porous membrane has a constant hydraulic conductivity of 1.0×10^{-5} m/s as it remained saturated throughout the test. The HCFs predicted from the parameters of the WRCs using the van Genuchten-Mualem model (van Genuchten 1980) (Eq. 2) are shown in both figures. A reasonable match is observed between the predicted HCF and the measured HCF data, with R-squared values of approximately 0.85. It is much easier to predict the HCF from the

parameters of the WRC using Equation (2) than to measure it independently, so the reasonable match between the predicted and measured HCFs for organophilic clay blankets is a useful conclusion for practical analyses. Comparing the predicted HCFs in Figures 9(a) and 9(b), the HCF for the rinsed blanket with an effective confining stress of 5 kPa shows a wider range that starts from a higher hydraulic conductivity of 8.0×10^{-4} m/s. This is attributed to both the loss of fines during rinsing and the lower effective confining stress.

AIR PERMEABILITY RESULTS

The gas ebullition pressure was measured directly for the unrinsed and rinsed specimens by increasing the air pressure at the base of the specimen until reaching breakthrough (as detected by bubbles appearing in the tubing connected to the top of the specimen). Note that the high air-entry porous membrane was not used in the gas ebullition tests. In both tests, gas ebullition occurred at the same air pressure of 0.60 kPa. The magnitude of the gas ebullition pressure measured directly is the same as that inferred from the WRC of the rinsed specimen but is 0.08 kPa lower than that inferred from the WRC of the unrinsed specimen. The slightly lower gas ebullition pressure for the unrinsed specimen may have occurred due to preferential gas flow through a bundle of the needle-punched fibers or a thinner section of the organophilic clay. The role of preferential flow paths like these on the gas ebullition pressure may be different when slowly drawing water from the specimen during measurement of the WRC and when gradually increasing the gas pressure on the bottom boundary of the specimen. Nonetheless, the similarity of the gas ebullition pressures from the indirect and direct approaches confirms that both approaches may be used to obtain the gas ebullition pressures as part of a sediment capping permitting process.

After reaching the gas ebullition pressure in the test on the unrinsed specimen, the gas pressure was maintained and the air flow volume as a function of time was measured by forcing water from

one reservoir into another. The air flow volume and pressure gradient measured as a function of time during this test are shown in Figure 10(a). Although the presentation of results in this figure makes it seem that there was a delay in the outflow of air after reaching breakthrough, the outflow data was not recorded until after 2 minutes for the first pressure difference of 0.6 kPa, and until after 8 minutes for the second pressure difference of 0.9 kPa. Air flow was occurring through the blanket throughout the 16-minute experiment. For the first pressure gradient, the air flow volume passing through the specimen was observed to be linear with time. When the pressure gradient was increased a linear gas flow rate was still observed. The air flow rates and air pressure gradients at steady state are shown in Figure 10(b) for the two different applied air pressures. A linear relationship is observed, and the air permeability calculated from the results of both tests using Eq. (4) is 0.04 darcys.

The air permeability of the rinsed specimen under a lower effective stress was measured by applying a constant gas flow rate using a mass flow controller while measuring the pressure difference across the specimen using the differential pressure transducer. Using a mass flow controller permits the air flow rate to be maintained at a constant level. The air flow rate and the measured pressure difference across the specimen are shown in Figure 11(a). The measured pressure difference was variable in the first part of the test (up to 2 hours) possibly due to capillary effects during initial desaturation of the organophilic clay blanket that caused bubbles to rise and fall in the tubing, resulting in the variable pressure differences. It is also possible that breakthrough occurred through only a single pore of the specimen (i.e., a large void in the organophilic clay or a bundle of needle-punched fibers), leading to a concentration of the air flow through only a portion of the specimen area. The air flow was stopped after 3.5 hours, and the air flow rates were repeated in stages. More stable results were observed after this point, indicating that air flow may have been

occurring through multiple pathways across the specimen area. The applied air rates and equilibrium values of pressure difference for the final set of stages starting after 3.78 hours are shown in Figure 11(b). A nonlinear trend is noted, different from that observed in Figure 11(b). The nonlinearity may be due to the opening of additional air pathways through the specimen for higher air flow rates. The air permeability measured during application of low air flow rates is approximately 0.24 darcys, while application of higher flow rates the air permeability decreases to approximately 0.08 darcys. The average air permeability over the entire range of air flow rates is 0.16 darcys. The air permeability values measured in this test are 2 to 7 times greater than the value measured for the un-rinsed organophilic clay blanket under an effective stress of 20 kPa.

CONCLUSIONS

In this study, the air-entry pressure of initially water-saturated organophilic clay blankets was indirectly evaluated through the water retention curve and directly through ebullition experiments which also permit evaluation of gas permeability. This comparison was performed using tests on organophilic clay blanket specimens in the as-received condition under an effective confining stress of 20 kPa to represent a thicker overburden layer and in a rinsed condition to represent the case that loose fines are removed by water flow under a lower effective confining stress of 5 kPa to represent a thin overburden layer. A key conclusion from this study is that the indirect approach to estimate the air-entry suction from the WRC provides similar results to gas ebullition experiments. This is important as gas ebullition experiments are complicated to perform due to issues with side-wall leakage and the difficulty to consider the effects of flow through preferential pathways, so the availability of a reliable indirect method is useful in the development of specifications for organophilic clay barriers used in sediment capping systems.

The results from the indirect and direct approaches indicate that the organophilic clay blanket specimens have air-entry suctions between 0.60 and 0.68 kPa, with a slightly greater air-entry suction for the specimen under unrinsed conditions and a higher overburden stress. As rinsing likely affects the fines content in the blanket which is associated with the shape of the WRC at high suctions, it is assumed that the compression of the nonwoven geotextile fibers under the higher effective confining stress contributed to a more tightly-packed organophilic clay and denser geotextile fiber structure leading to the higher air-entry suction. This may imply that the use of thicker overburden and armor layers may have a slight negative effect on the air-entry suction and hydraulic properties, although the positive effects of a greater vertical effective stress outweigh the increase in the ebullition pressure. The results from both the direct and indirect approaches indicate that organophilic clay blankets should be used in conjunction with an overburden of coarse material that applies a vertical total stress greater than the blanket's air-entry suction of approximately 0.6 kPa to prevent uplift of the blanket. This vertical total stress corresponds to the surcharge associated with a layer of poorly graded sand having a unit weight of 15 kN/m³ and a thickness of approximately 0.04 m. This thickness is relatively small, which is consistent with the goal of using a lightweight blanket in a sediment capping system. It should be emphasized that further testing is needed to evaluate possible changes in ebullition pressure if the organophilic clay blanket absorbs organic contaminants from the underlying sediment, which will lead to a reduction in the pore size distribution of the blanket.

Although definitive conclusions regarding the independent effects of effective confining stress and rinsing due to the limited number of tests presented in this study, some preliminary conclusions can be drawn from the flow processes in the tests reported in this study. The hydraulic conductivities for both rinsed and unrinsed specimens in saturated conditions was observed to

decrease with time, with a greater decrease for the unrinsed specimen, likely due to redistribution of particles under the seepage force applied during testing. The hydraulic conductivity was not observed to stabilize after at least 4 days of steady flow. The rinsed specimen under a lower effective confining stress had a hydraulic conductivity that was two orders of magnitude greater than the unrinsed specimen under a higher effective confining stress. The results indicate that rinsing leads to a loss of some fines, causing an increase in hydraulic conductivity, while greater effective stresses lead to compression of the voids causing a decrease in hydraulic conductivity. Similar effects of effective stress were observed for the air permeability. The air permeability values for the rinsed specimen under a low effective confining stress are 2 to 7 times greater than the air permeability measured for the unrinsed specimen under an effective stress of 20 kPa.

ACKNOWLEDGMENTS

Support from CETCO® is gratefully acknowledged, along with reviews from John Allen and Rob Vallorio. The views in this paper are those of the authors alone.

NOTATION

Basic SI units are given in parentheses.

k	Hydraulic conductivity under unsaturated conditions (m/s)
k_{sat}	Hydraulic conductivity under saturated conditions (m/s)
S_e	Effective saturation (m^3/m^3)
S	Degree of saturation (m^3/m^3)
S_{res}	Residual saturation (m^3/m^3)
α_{vg}	van Genuchten (1980) WRC model fitting parameter (kPa^{-1})
n_{vG}	van Genuchten (1980) WRC model fitting parameter (dimensionless)
m	van Genuchten (1980) WRC model fitting parameter (dimensionless)

492	ψ	Matric suction (kPa)
493	ψ_a	Air-entry suction (kPa)
494	τ	Tortuosity factor (dimensionless)
495	V	Outflow volume at a given time (m^3)
496	V_f	Final outflow volume (m^3)
497	H	Specimen height (m)
498	γ_w	Unit weight of water (kN/m^3)
499	D	Diffusivity (m^2/s)
500	θ	Volumetric water content (m^3/m^3)
501	θ_{sat}	Volumetric water content at saturation (m^3/m^3)
502	θ_{res}	Volumetric water content at saturation (m^3/m^3)
503	σ'	Effective confining stress
504	Q_{av}	Average volumetric flow rate of air (m^3/s)
505	ΔP	Applied pressure difference (kPa)
506	k_a	Air permeability (darcys)
507	A	Specimen area (m^2)
508	μ	Air viscosity (kPa-s)

509 ABBREVIATIONS

510	WRC	Water retention curve
511	HCF	Hydraulic conductivity function

512 REFERENCES

513 Alshawabkeh, A.N., Rahbar, N., and Sheahan, T. (2005). "A model for contaminant mass flux in
514 capped sediment under consolidation." Journal of Contaminant Hydrology, 78(3), 147-165.

515 Alsherif, N.A. and McCartney, J.S. (2015). "Nonisothermal behavior of compacted silt at low
 516 degrees of saturation." *Géotechnique*. 65(9), 703-716. DOI: 10.1680/geot./14 P 049.
 517 ASTM D6836. Standard Test Methods for Determination of the Soil Water Characteristic Curve
 518 for Desorption Using Hanging Column, Pressure Extractor, Chilled Mirror Hygrometer, or
 519 Centrifuge. ASTM International. West Conshohocken, PA.
 520 ASTM D7664. Standard Test Methods for Measurement of Hydraulic Conductivity of Unsaturated
 521 Soils. ASTM International. West Conshohocken, PA.
 522 Benson, C.H., Jo, H.Y., and Musso, T. (2015). "Hydraulic conductivity of Organoclay and
 523 Organoclay-sand mixtures to fuels and organic liquids." *Journal of Geotechnical and*
 524 *Geoenvironmental Engineering*. 141(2), 04014094.
 525 Chattopadhyay, S., Lal, V., and Foote, E. (2010). "Bench-scale evaluation of gas ebullition on the
 526 release of contaminants from sediments." EPA/600/R-10/062.
 527 Ebrahimi, A., Viswanash, M., Zhu, M., and Beech, J.F. (2014). "Methodology to evaluate
 528 geotechnical stability of a subaqueous cap placed on soft sediments." ASCE, Geo-Chicago
 529 2014.
 530 Ebrahimi, A., Erten, M.B., Carlson, C., Coraspe, T., Zhu, M., and Beech, J.F. (2016). "An
 531 integrated subsurface investigation for sediment capping projects." ASCE, Geo-Chicago 2016.
 532 Erten, M.B., Reible, D.D., Gilbert, R.B., and El Mohtar, C.S., "The performance of organoclay on
 533 nonaqueous phase liquid contaminated sediments under anisotropic consolidation." *Contaminated Sediments: Restoration of Aquatic Environment* on May 23-25, 2012 in
 534 Montreal, Quebec, Canada; STP 1554, C.N. Mulligan and S.S. Li, Editors, pp. 32-44,
 535 dOi:10.1520/STP104214, ASTM International. West Conshohocken, PA 2012.
 536

537 Eun, J. and Tinjum, J.M. (2012a) "Variation in air entry suction of nonwoven geotextiles with pore
538 size distribution." 5th Asia-Pacific Conference on Unsaturated Soils, ISSMGE, Nov. 14-16,
539 2011, Pattaya, Thailand.

540 Eun, J. and Tinjum, J.M. (2012b). "Unsaturated transport of ebullition gas through sediment
541 capping geotextiles and sand." 5th Asia-Pacific Conference on Unsaturated Soils. ISSMGE,
542 Nov. 14-16, 2011, Pattaya, Thailand.

543 Gu, B.W., Lee, C.G., Lee, T.G., and Park, S.J. (2017). "Evaluation of sediment capping with
544 activated carbon and nonwoven fabric mat to interrupt nutrient release from lake sediments."
545 Science of the Total Environment, 599-600, 413 – 421.

546 Lampert, D.J. and Reible, D.D. (2009). "An analytical modeling approach for evaluation of
547 capping of contaminated sediments." Soil and Sediment Contamination: An International
548 Journal. 18(4), 470-488

549 Lo, I.M.C. and Yang, X. "Use of organophilic clay as secondary containment for gasoline storage
550 tanks." J. Environ. Eng. 127(2), 154-161.

551 Locat, J., Cloutier, R.G., Chaney, R., and Demars, K. (2003). "Contaminated sediments:
552 characterization, evaluation, mitigation/restoration and management strategy performance."
553 ASTM, STP 1442 ISBN: 0-8031-3466-5.

554 McCartney, J.S. and Znidarčić, D. (2010). "Test system for hydraulic properties of unsaturated
555 nonwoven geotextiles." Geosynthetics International. 17(5), 355-363.

556 McCartney, J.S. and Zornberg, J.G. (2010). "Effect of cyclic wetting and drying on the formation
557 of a capillary break between soil and geosynthetic drainage layers." Canadian Geotechnical
558 Journal. 47(11), 1201-1213.

559 McLinn, E.L. and Stolzenburg, T.R. (2009a). "Ebullition-facilitated transport of manufactured gas
 560 plant tar from contaminated sediment." *Environmental Toxicology and Chemistry*, 28(11),
 561 2298–2306.

562 McLinn, E.L. and Stolzenburg, T.R. (2009b). "Investigation of NAPL transport through a model
 563 sand cap during ebullition." *Remediation Journal*, 19(2), 63-69.

564 Mohan, R.K., Brown, M.P., and Barnes, C.R. (2000). "Design criteria and theoretical basis for
 565 capping contaminated marine sediments." *Applied Ocean Research*, 22, 85-93.

566 Mualem, Y. (1976). "A new model for predicting the hydraulic conductivity of unsaturated porous
 567 media." *Water Resources Res.*, 12, 513-522.

568 Nahlawi, H., Bouazza, A., and Kodikara, J., (2007). "Characterisation of geotextiles water retention
 569 using a modified capillary pressure cell." *Geotextiles and Geomembranes* 25 (3), 186–193.

570 Olsta, J. (2010). "In-situ capping of contaminated sediments with organophilic clay." ASCE, 12th
 571 Triannual International Conference on Ports. doi.org/10.1061/41098(368)62.

572 Palermo, M.R. (1998). "Design considerations for in-situ capping of contaminated sediments."
 573 *Water Sci. Technol.* 37, 315.

574 Paul, D., Zeng, Q., Yu, A., and Lu, G. (2005). "The interlayer swelling and molecular packing in
 575 organophilic clays." *J. Colloid Interface Sci.* 292, 462-468.

576 Perele, L.W. (2010). "Review: In situ and bioremediation of organic pollutants in aquatic
 577 sediments" *Journal of Hazardous Materials*, 177, 81-89.

578 Reible, D.D., Hayes, D., Lue-Hing, C., Patterson, J., Bhowmik, N., and Johnson. M. (2003).
 579 "Comparison of the long-term risks of removal and in-situ management of contaminated
 580 sediments in the Fox River." *Journal of Soil Contamination*. 12(3), 325–344.

581 Reible, D., Lampert, D., Constant, D., Mutch, R.D.J., and Zhu, Y. (2006). "Active capping
 582 demonstration in the Anacostia River, Washington, D.C." *Remediation Journal*, 17(1) 39-53.
 583 DOI: 10.1002/rem.20111.

584 van Genuchten, M. (1980). "A closed-form equation for predicting the hydraulic conductivity of
 585 unsaturated soils." *Soil Sci. Soc. Am. J.*, 44, 892–898.

586 Yuan, Q., Valsaraj, K.T., Reible, D.D., and Willson, C.S. (2007). "A laboratory study of sediment
 587 and contaminant release during gas ebullition." *Journal of the Air & Waste Management*
 588 *Association*. 57(9), 1103-1111

589 Yuan, Q., Valsaraj, K.T., and Reible, D.D. (2009). "A model for contaminant and sediment
 590 transport via gas ebullition through a sediment cap." *Environmental Engineering Science*, 26,
 591 9 1381-1391 (2009)

592 Zeller, C. and Cushing, B. (2006). "Panel discussion: remedy effectiveness: what works, what
 593 doesn't?" *Integrated Environmental Assessment and Management*, 2(1), 75–79.

594 Zhang, C., Zhu, M., Zeng, G., Yu, Z., Cui, F., Yang, Z., and Shen, L. (2016). "Active capping
 595 technology: a new environmental remediation of contaminated sediment." *Environmental*
 596 *Science and Pollution Research International*; Heidelberg, 23(5), 4370–4386.

597 Znidarčić, D., Illangasekare, T., and Manna, M. (1991). "Laboratory testing and parameter
 598 estimation for two-phase flow problems." *Proceedings of the Geotechnical Engineering*
 599 *Congress*, Boulder, CO, McLean, F.G., Campbell, D.A. and Harris, D. W., Editors, ASCE,
 600 New York, pp. 1078–1089.

601 Zornberg, J.G., Bouazza, A., and McCartney J.S. (2010). "Geosynthetic capillary barriers: State-
 602 of-the-knowledge." *Geosynthetics International*. 17(5), 273–300.

Table 1. Characteristics of the upper and lower carrier geotextiles of the organophilic clay blanket tested.

Variable	Units	Nonwoven cap geotextile	Nonwoven carrier geotextile
Color		White	Black
G_s , geotextiles		0.92	0.92
Fiber density	kg/m ³	920	920
Mass per unit area	kg/m ²	0.20	0.20
Thickness	mm	2.5	2.0
Porosity		0.913	0.891

Table 2. Hydraulic properties of organophilic clay blanket specimens measured under different effective stresses and rinsing conditions.

Parameter	Un-rinsed specimen	Rinsed specimen
σ' (kPa)	20	5
θ_{sat} for drying path WRC	0.97	0.99
θ_{res} for drying path WRC	0.00	0.00
α_{vG} for drying path WRC (kPa ⁻¹)	0.78	1.20
n_{vG} for drying path WRC	2.46	2.50
k_{sat} under applied σ' (m/s)	9.0×10^{-7}	3.0×10^{-5}

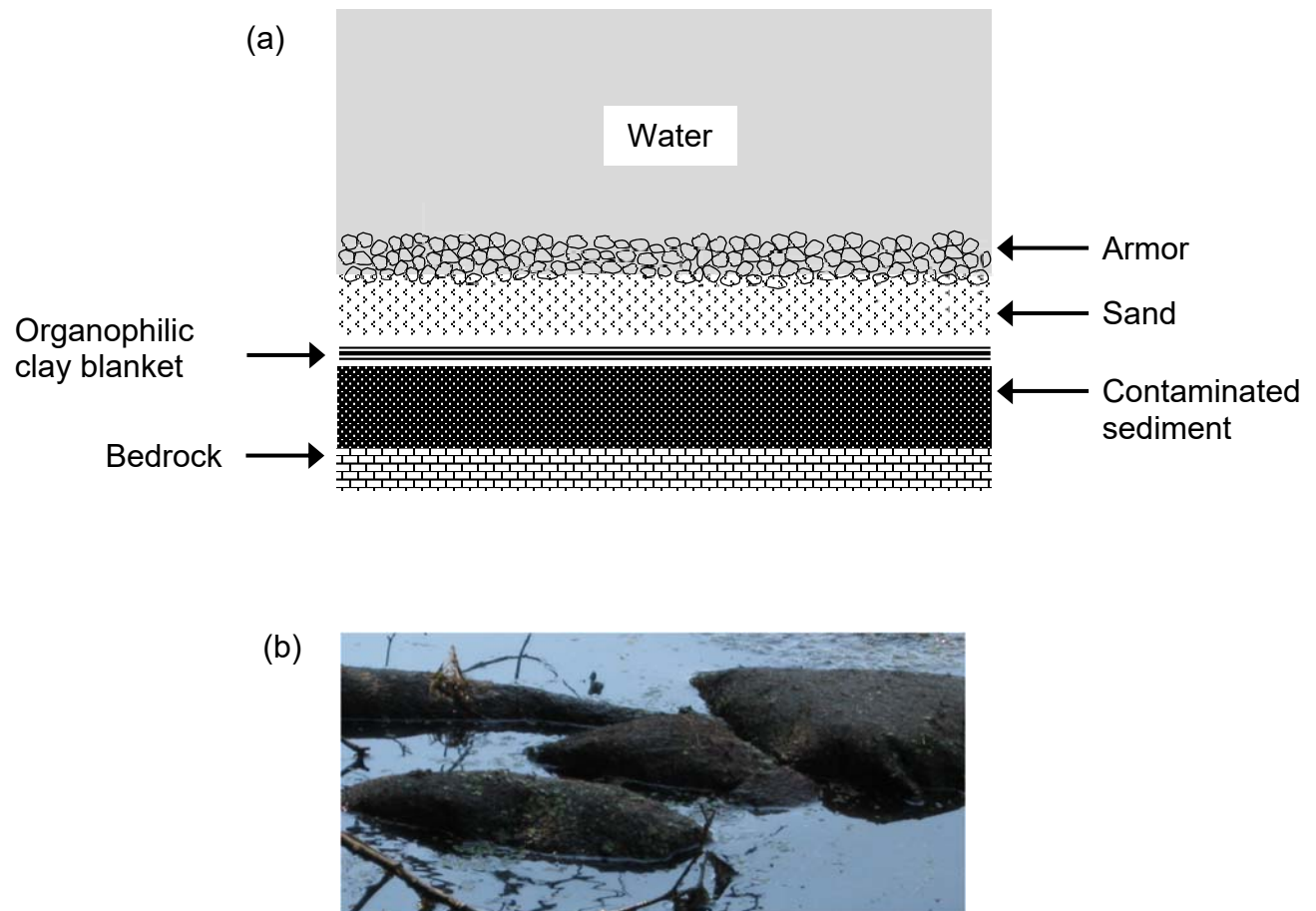


Figure 1. Schematic of sediment capping. (a) Gas ebullition from the capping and (b) Uplift failure of an organophilic clay blanket installed atop river sediments due to gas ebullition effects.

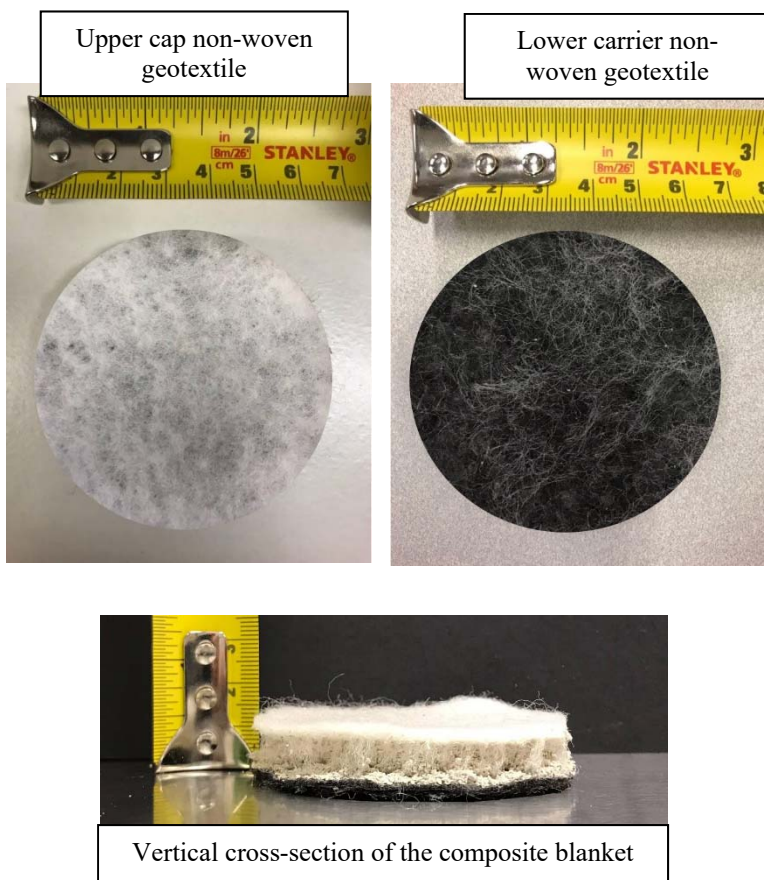


Figure 2. Organophilic clay blanket.

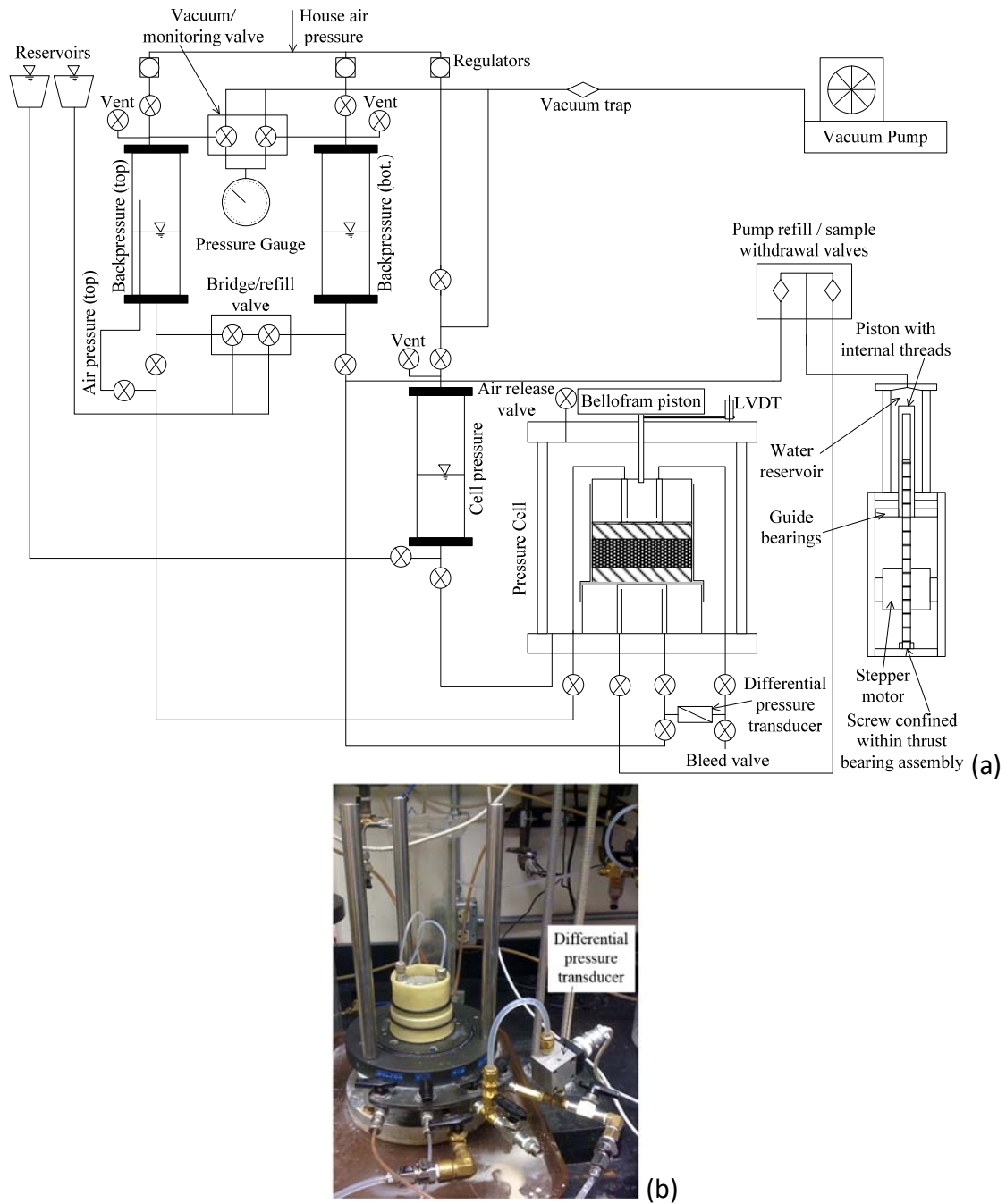


Figure 3. Flow pump permeameter used for measurement of hydraulic properties of organophilic clay blankets: (a) Schematic; (b) Picture of setup.

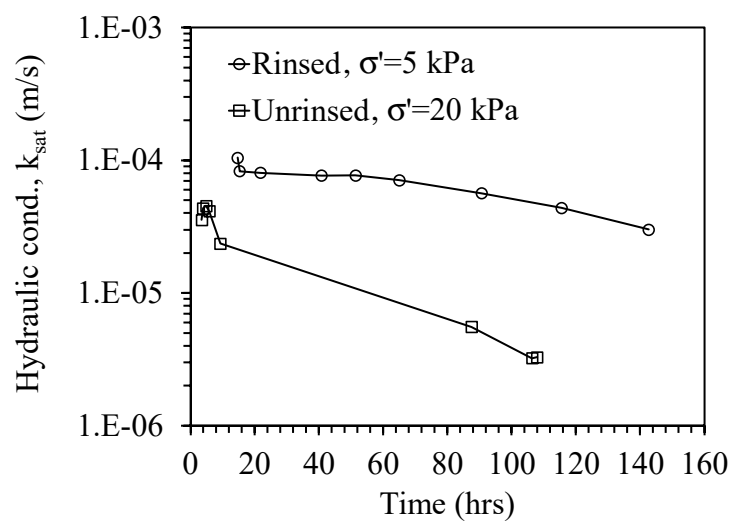


Figure 4. Hydraulic conductivity under saturated conditions as a function of time for unrinsed organophilic clay blanket with $\sigma' = 20$ kPa and rinsed organophilic clay blanket with $\sigma' = 5$ kPa.

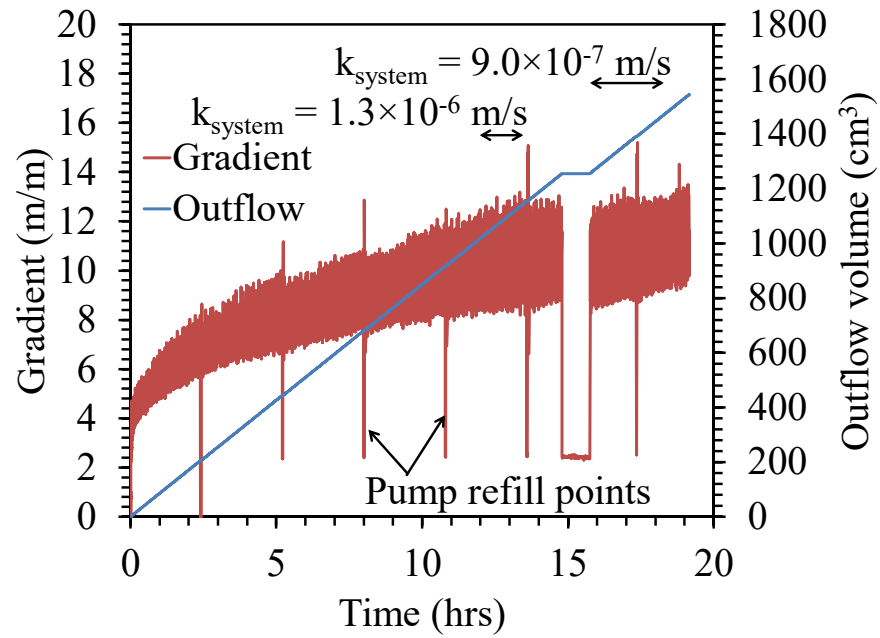


Figure 5. Flow tests to measure the saturated hydraulic conductivity of the organophilic clay blanket and high air entry porous membrane assembly (unrinsed organophilic clay blanket with $\sigma' = 20 \text{ kPa}$).

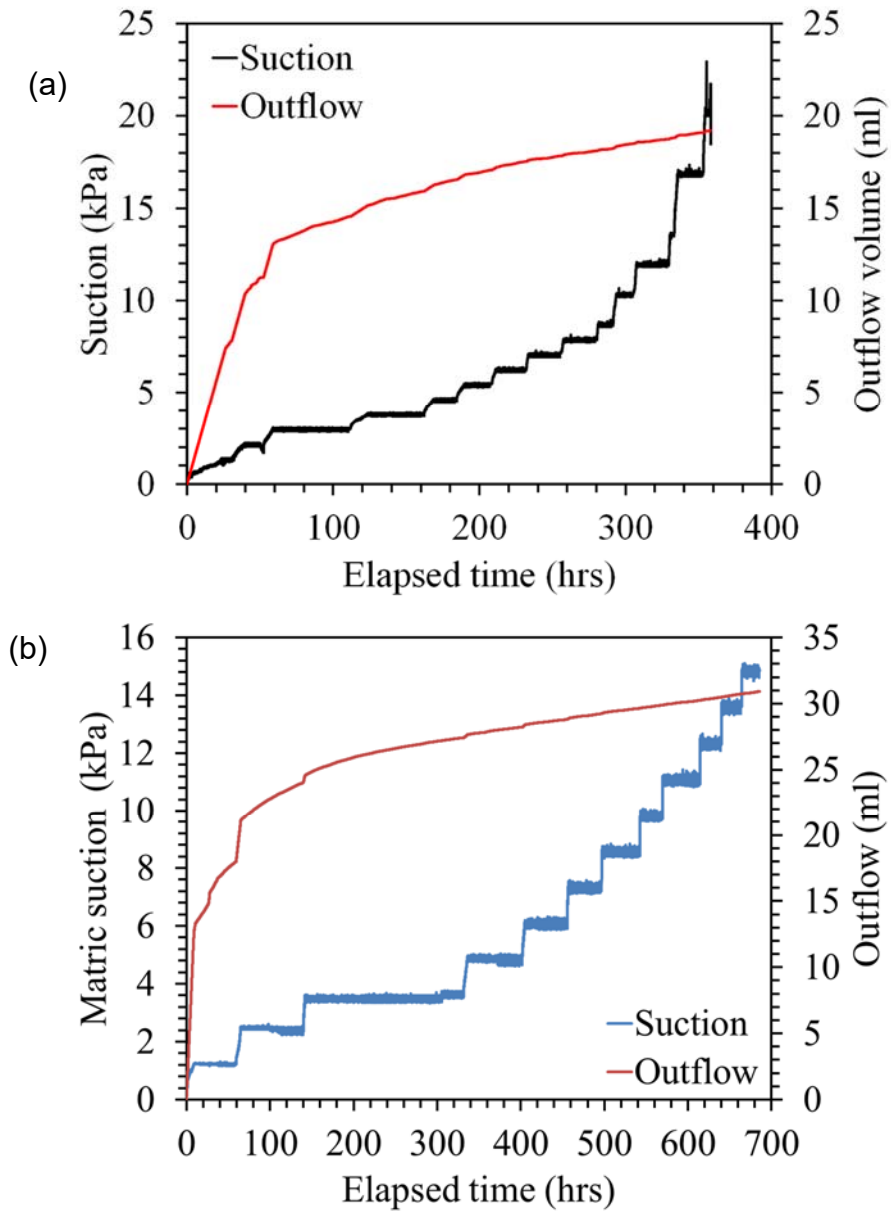


Figure 6. Outflow and suction as a function of time: (a) Unrinsed organophilic clay blanket with $\sigma' = 20$ kPa; (b) Rinsed organophilic clay blanket with $\sigma' = 5$ kPa.

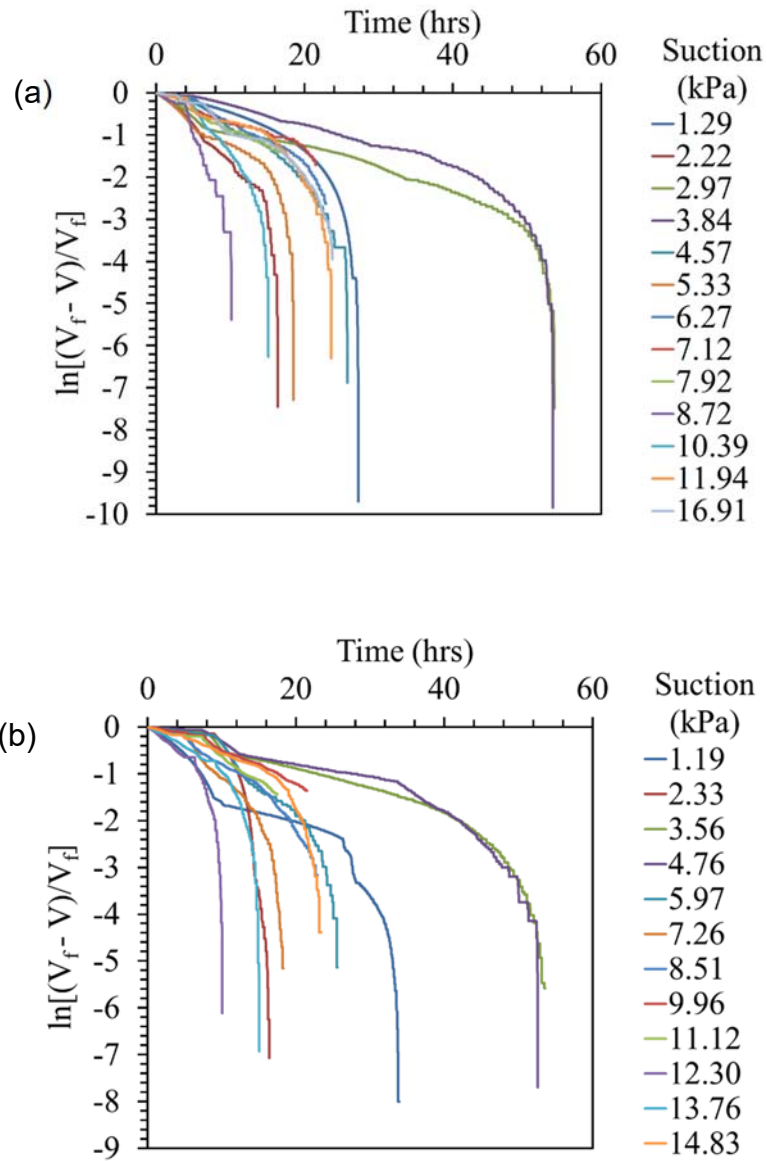


Figure 7. Transformed transient outflow curves for different suction increments: (a) Unrinsed organophilic clay blanket with $\sigma' = 20$ kPa; (b) Rinsed organophilic clay blanket with $\sigma' = 5$ kPa.

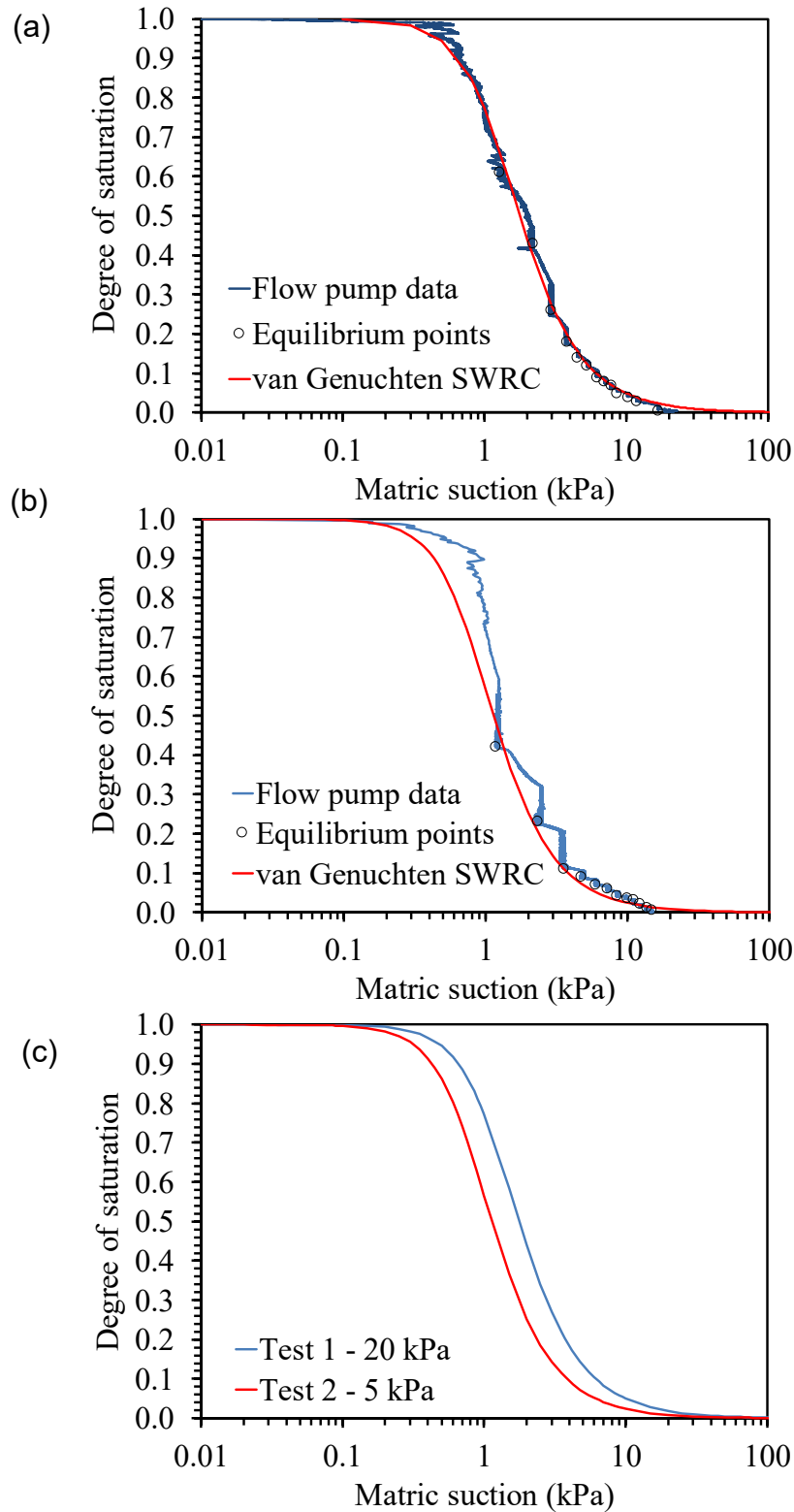


Figure 8. Experimental and fitted van Genuchten (1980) WRCs: (a) Test 1: Unrinsed organophilic clay blanket with $\sigma' = 20$ kPa; (b) Test 2: Rinsed organophilic clay blanket with $\sigma' = 5$ kPa; (c) Comparison of WRC curves for the two organophilic clay blanket specimens.

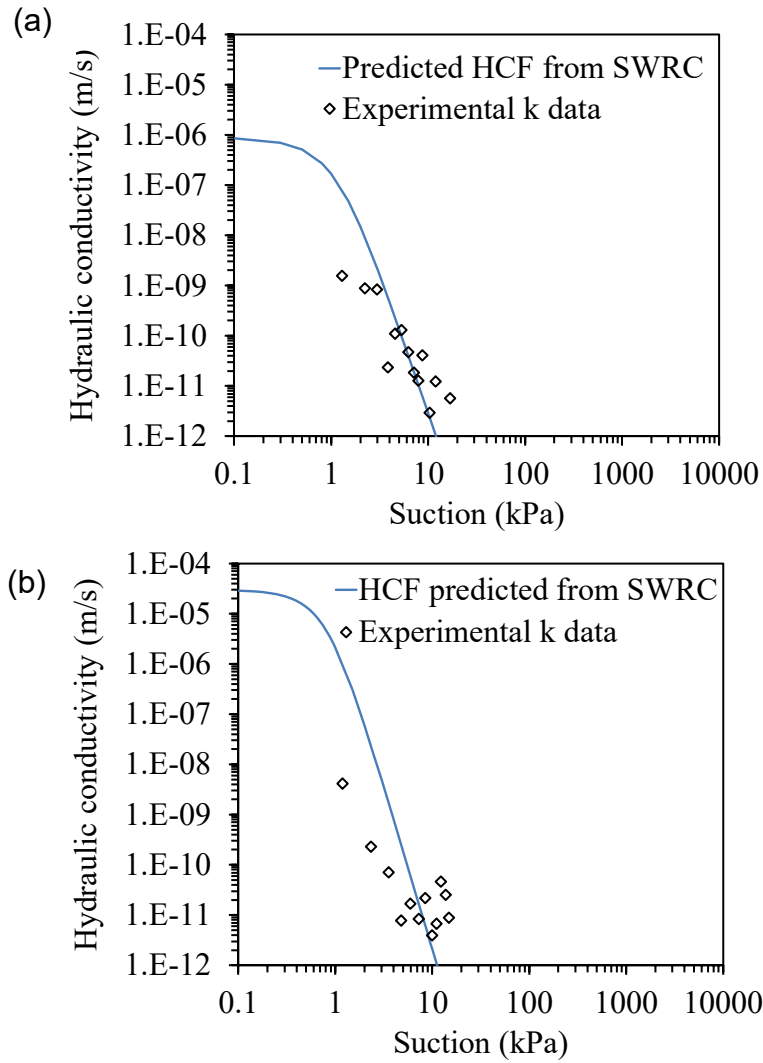


Figure 9. Comparison of the van Genuchten-Mualem (1980) HCF predicted from the SWRC with measured k data: (a) Unrinsed organophilic clay blanket with $\sigma' = 20$ kPa; (b) Rinsed organophilic clay blanket with $\sigma' = 5$ kPa.

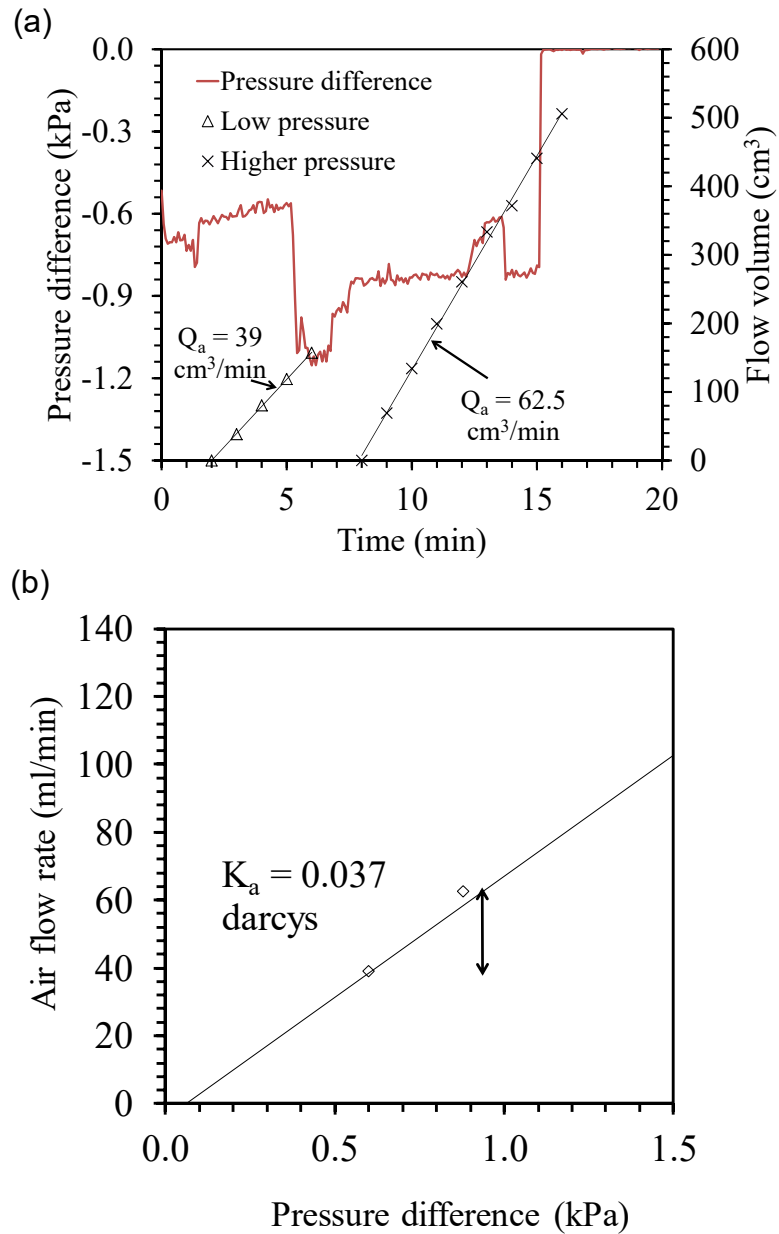


Figure 10. Air permeability of an unrinsed organophilic clay blanket ($\sigma' = 20$ kPa) (a) Applied air flow volume and measured pressure difference across an unrinsed organophilic clay blanket as a function of time; (b) Air flow rates versus pressure differences at different steady-state conditions.

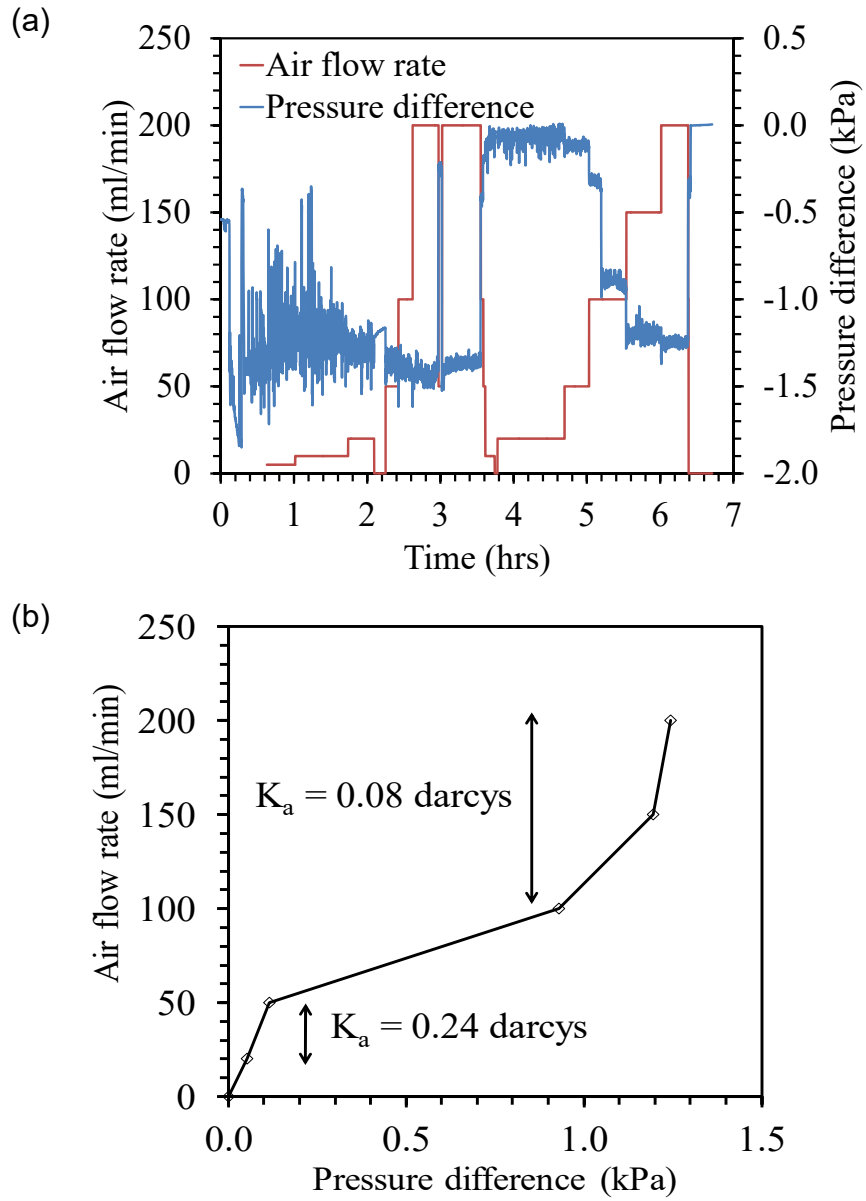


Figure 11. Air permeability of a rinsed organophilic clay blanket ($\sigma' = 5$ kPa) (a) Air flow volume and pressure difference across a rinsed organophilic clay blanket as a function of time; (b) Equilibrium air flow rate versus pressure difference.